

Supplementary Figures

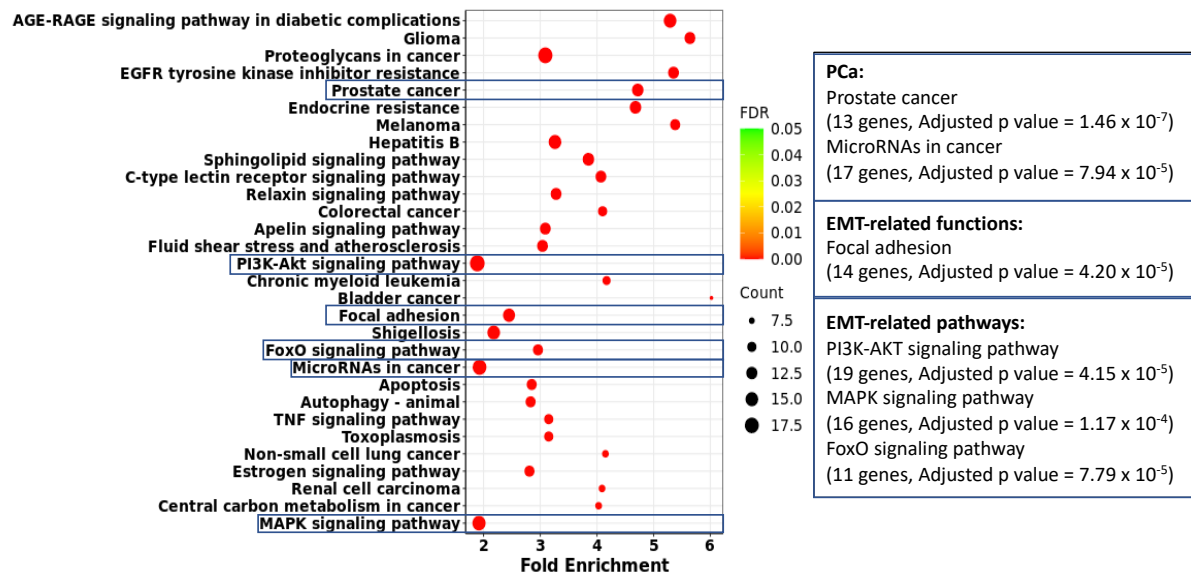


Figure S1. Bubble plot of KEGG functional enrichment analysis of miR-143-3p targets generated by CancerMIRNome.

EMT-related signaling pathways:

“PI3K-AKT”: https://dbemt.bioinfo-minzhao.org/literature_highlight.cgi?gene=207 (accessed on 10 May 2023).

“MAPK”: https://dbemt.bioinfo-minzhao.org/literature_highlight.cgi?gene=5594 (accessed on 10 May 2023).

“FoxO”: https://dbemt.bioinfo-minzhao.org/literature_highlight.cgi?gene=2308. (accessed on 10 May 2023).

FDR = False Discovery Rate

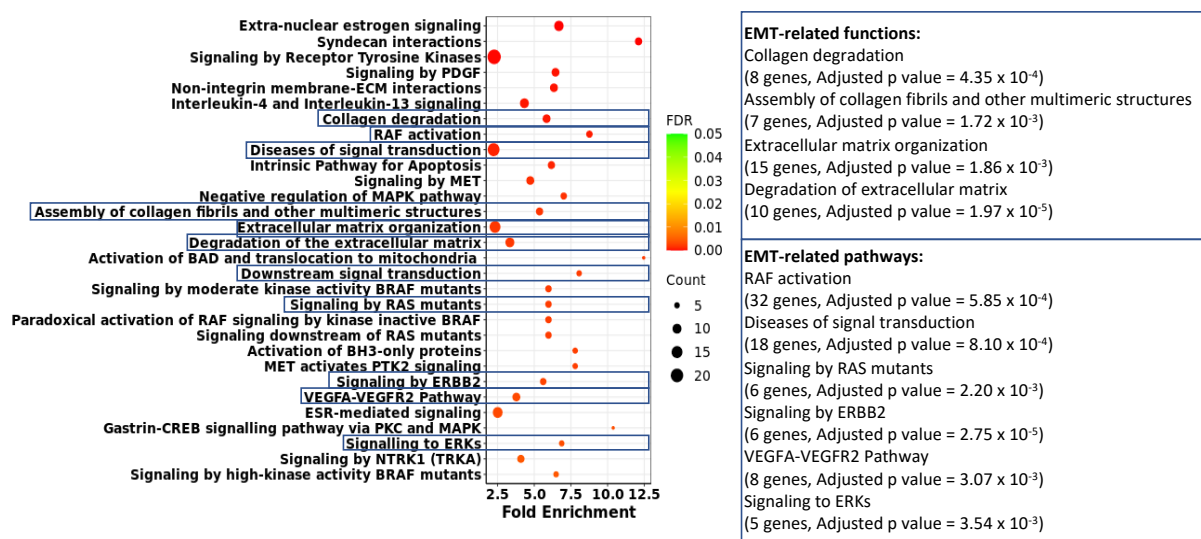


Figure S2. Bubble plot of REACTOME functional enrichment analysis of miR-143-3p targets generated by CancerMIRNome.

EMT-related signaling pathways:

“RAF”: https://dbemt.bioinfo-minzhao.org/literature_highlight.cgi?gene=5894 (accessed on 12 May 2023).

“RAS”: https://dbemt.bioinfo-minzhao.org/literature_highlight.cgi?gene=3845 (accessed on 12 May 2023).

“ERBB3”: https://dbemt.bioinfo-minzhao.org/literature_highlight.cgi?gene=2064 (accessed on 12 May 2023).

“VEGFA-VEGFR2”: https://dbemt.bioinfo-minzhao.org/literature_highlight.cgi?gene=7422 (accessed on 12 May 2023).

“PI3K-AKT”: https://dbemt.bioinfo-minzhao.org/literature_highlight.cgi?gene=207 (accessed on 12 May 2023).

FDR = False Discovery Rate

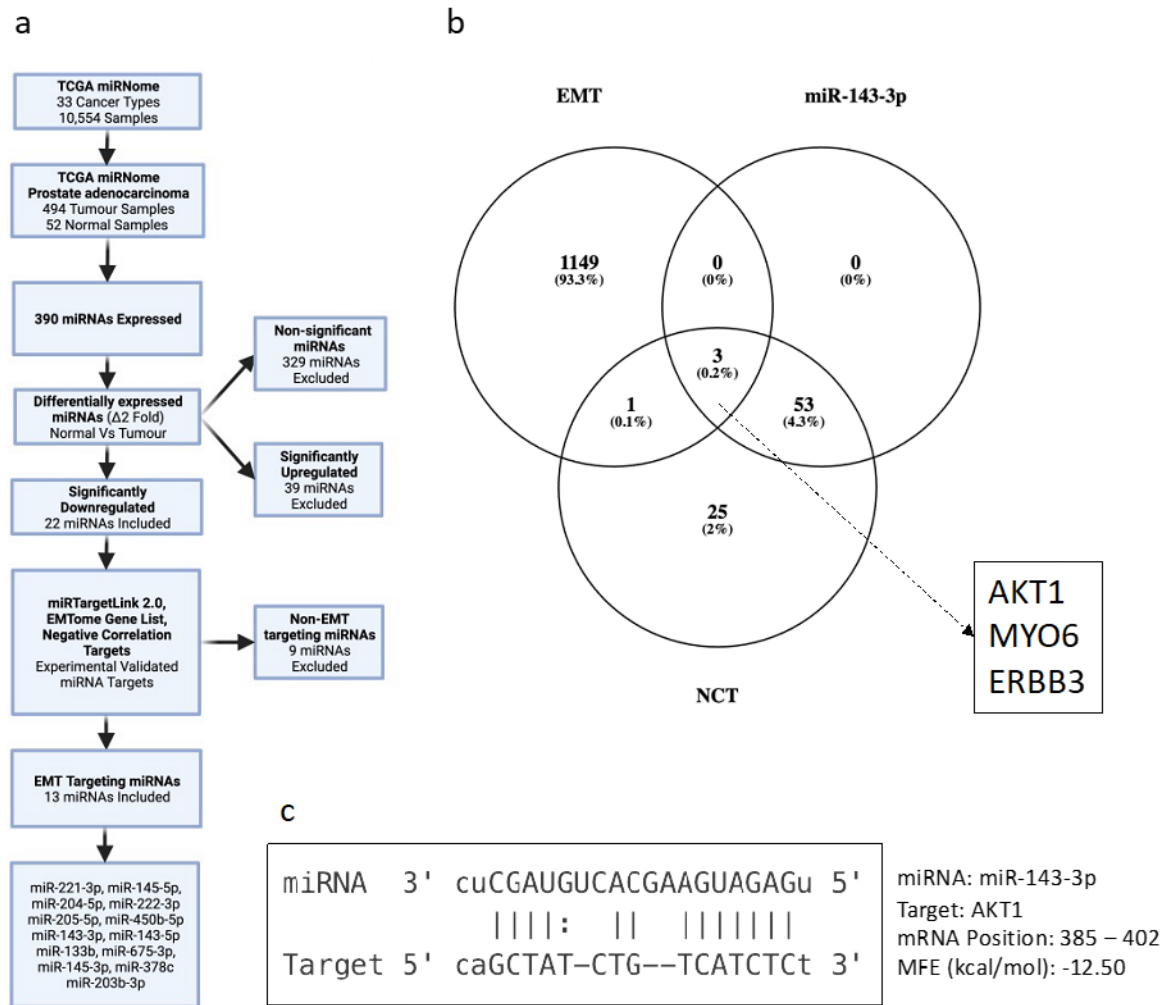


Figure S3. *In silico* selection of downregulated miRNAs in prostate cancer associated with EMT. (a) Selection process for identifying EMT associated miRNAs in prostate cancer. (b) Targets of the significantly downregulated miR-143-3p were predicted using miRTargetLink 2.0. Targets were cross-referenced to EMTome gene list and negative correlation targets in prostate cancer. (c) miR-TarBase computational prediction of miR-143-3p-AKT1 interaction. **EMT** = epithelial-to-mesenchymal transition; **NTC** = Negative Correlation Targets.

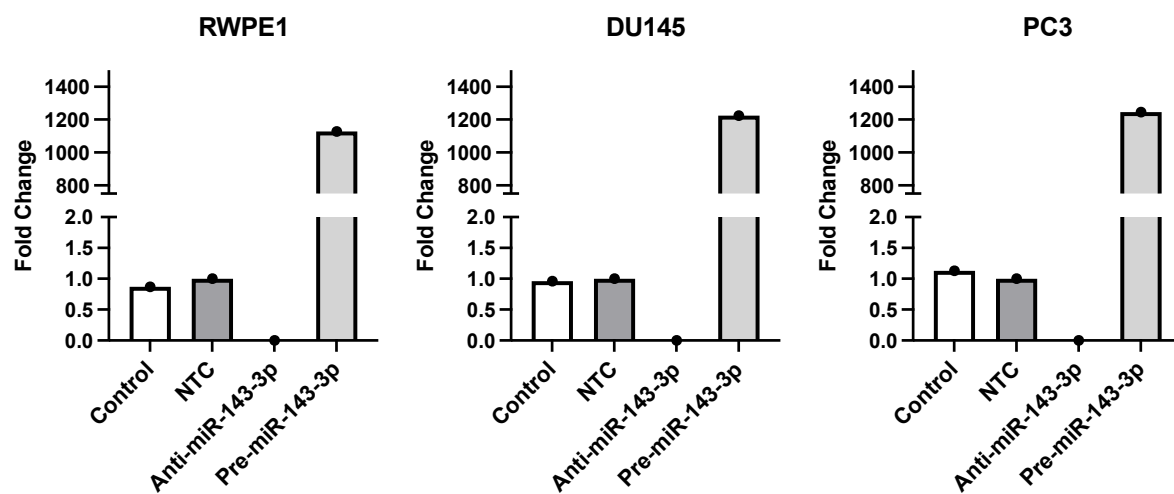


Figure S4: Confirmation of miR-143-3p overexpression and inhibition in prostate cell lines. ($n = 1$, housekeeping: snRNA U6).

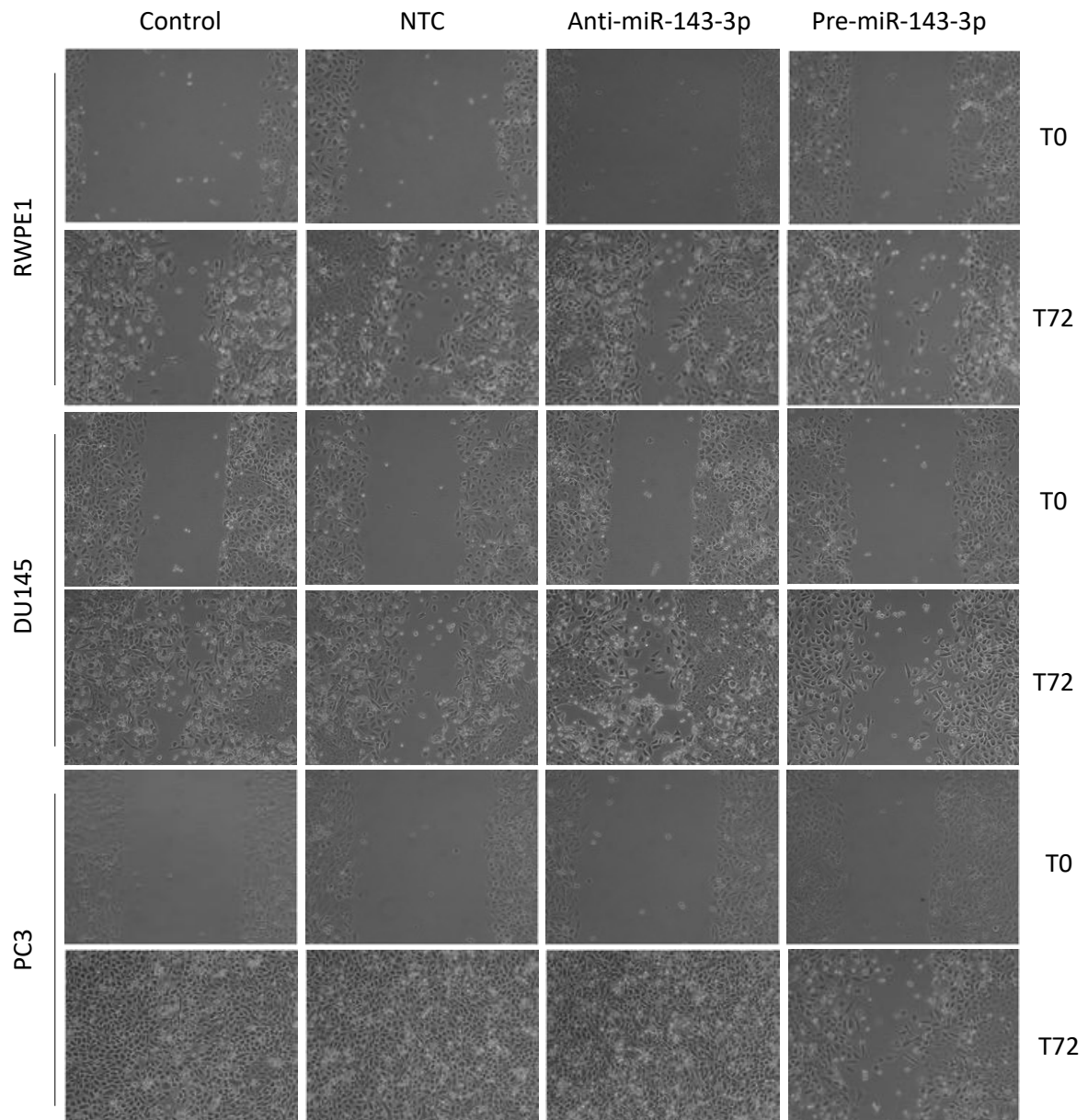


Figure S5: Representative images of wound-healing assay. miR-143-3p controls migratory capacity of RWPE1, DU145 and PC3 cell lines. Scratch assay performed at 72 hours post transfection using ImageJ software to quantify wound closure %. Pre-miR-Neg, Anti-miR-143-3p, Pre-miR-143-3p (25 nM). NTC = Non-targeting Control.

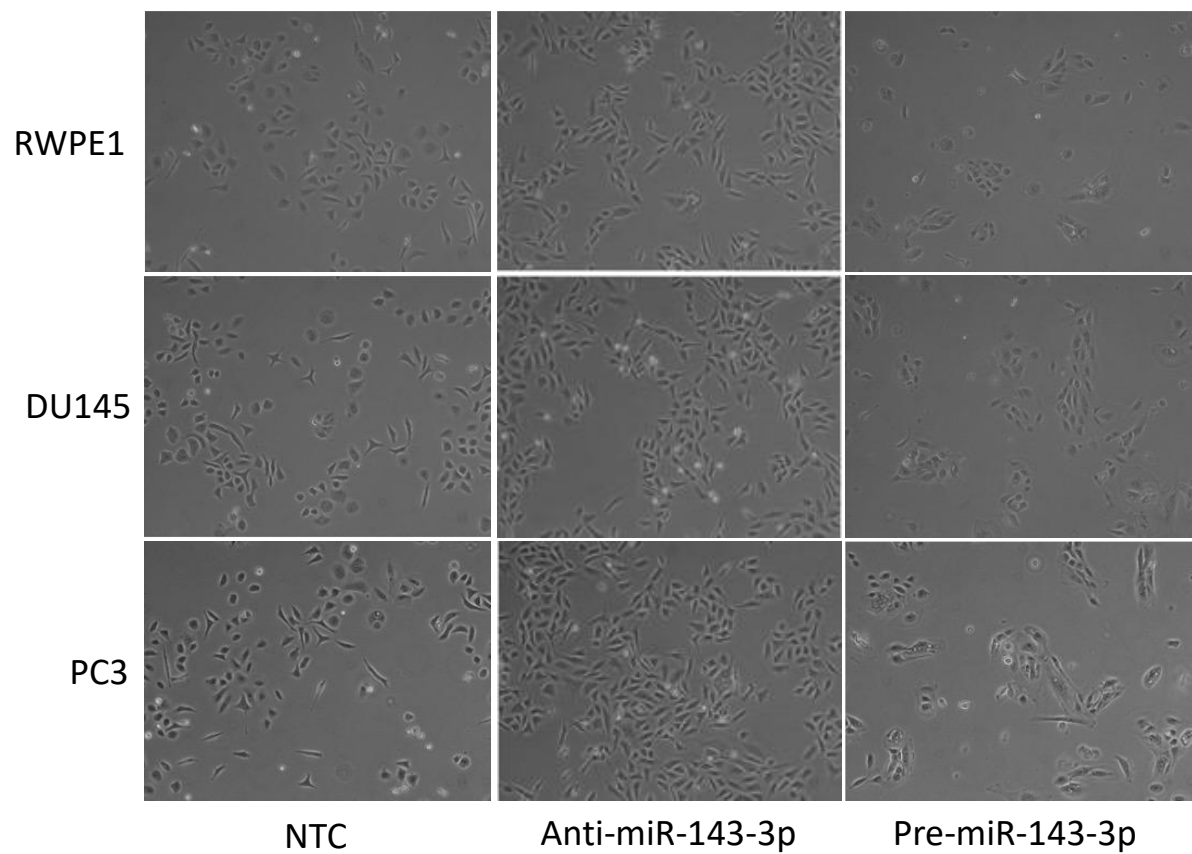


Figure S6: Representative images of clonogenicity assay. miR-143-3p alters colony forming capacity of RWPE1, DU145 and PC3 cell lines. Cell count performed using ImageJ software at 72 hours post transfection. Pre-miR-Neg, Anti-miR-143-3p, Pre-miR-143-3p (25 nM).

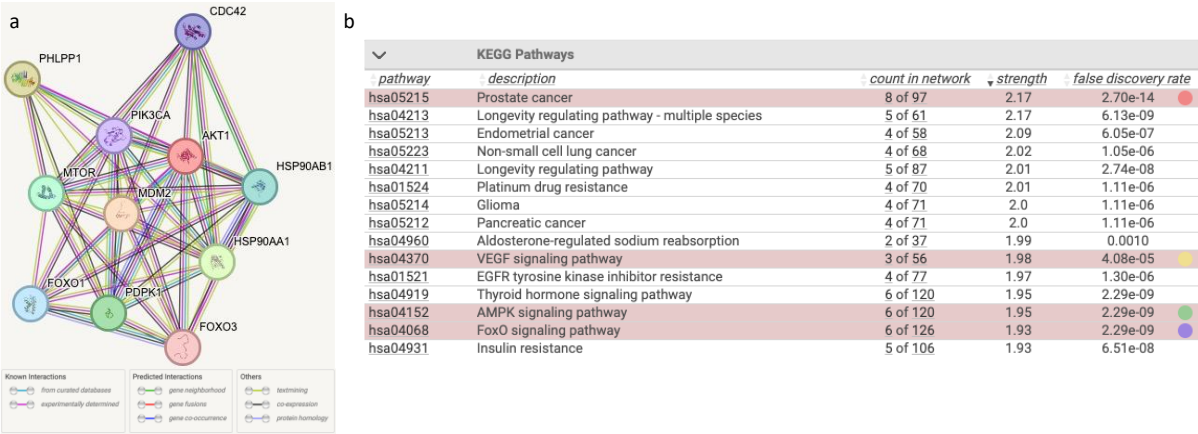


Figure S7. Network analysis of AKT1 protein interactions. (a) Visualization of network by String-DB Version 12. (b) KEGG Pathway analysis of the AKT1 network is significantly associated with prostate cancer and pathways related to EMT.

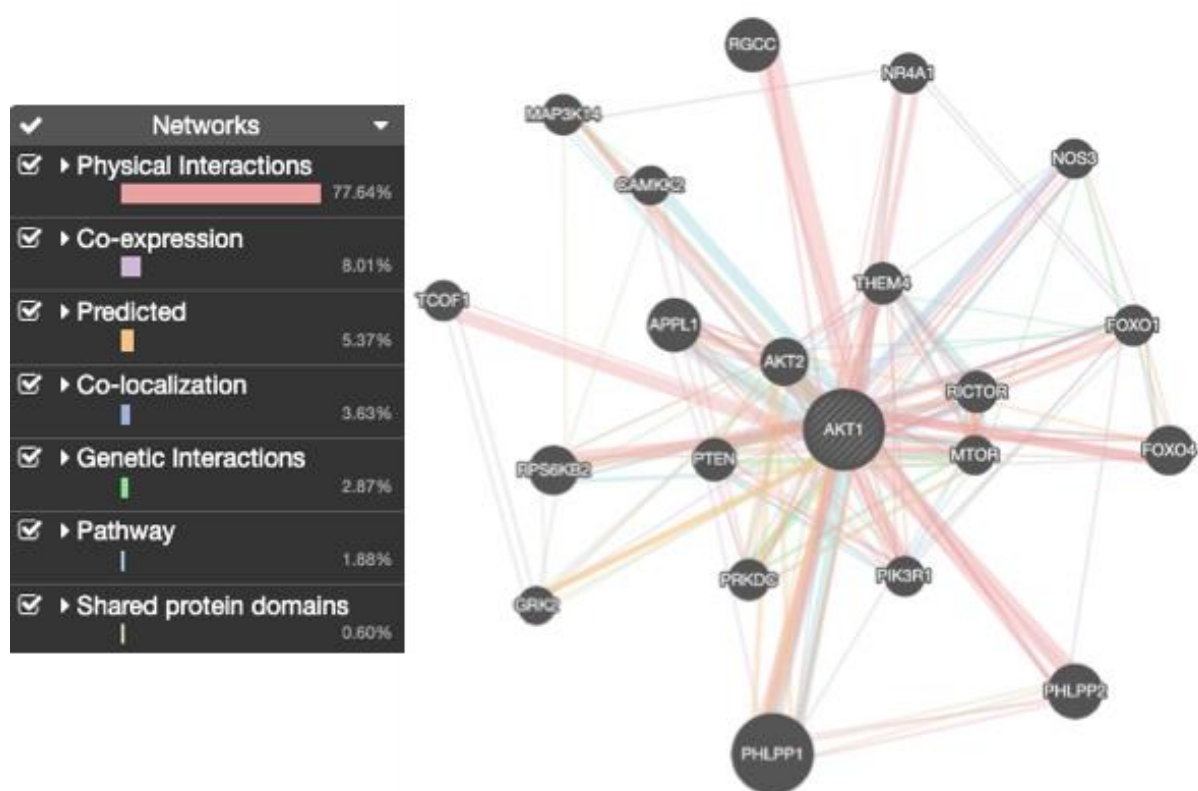


Figure S8. GeneMANIA network analysis of AKT1 gene interactions.

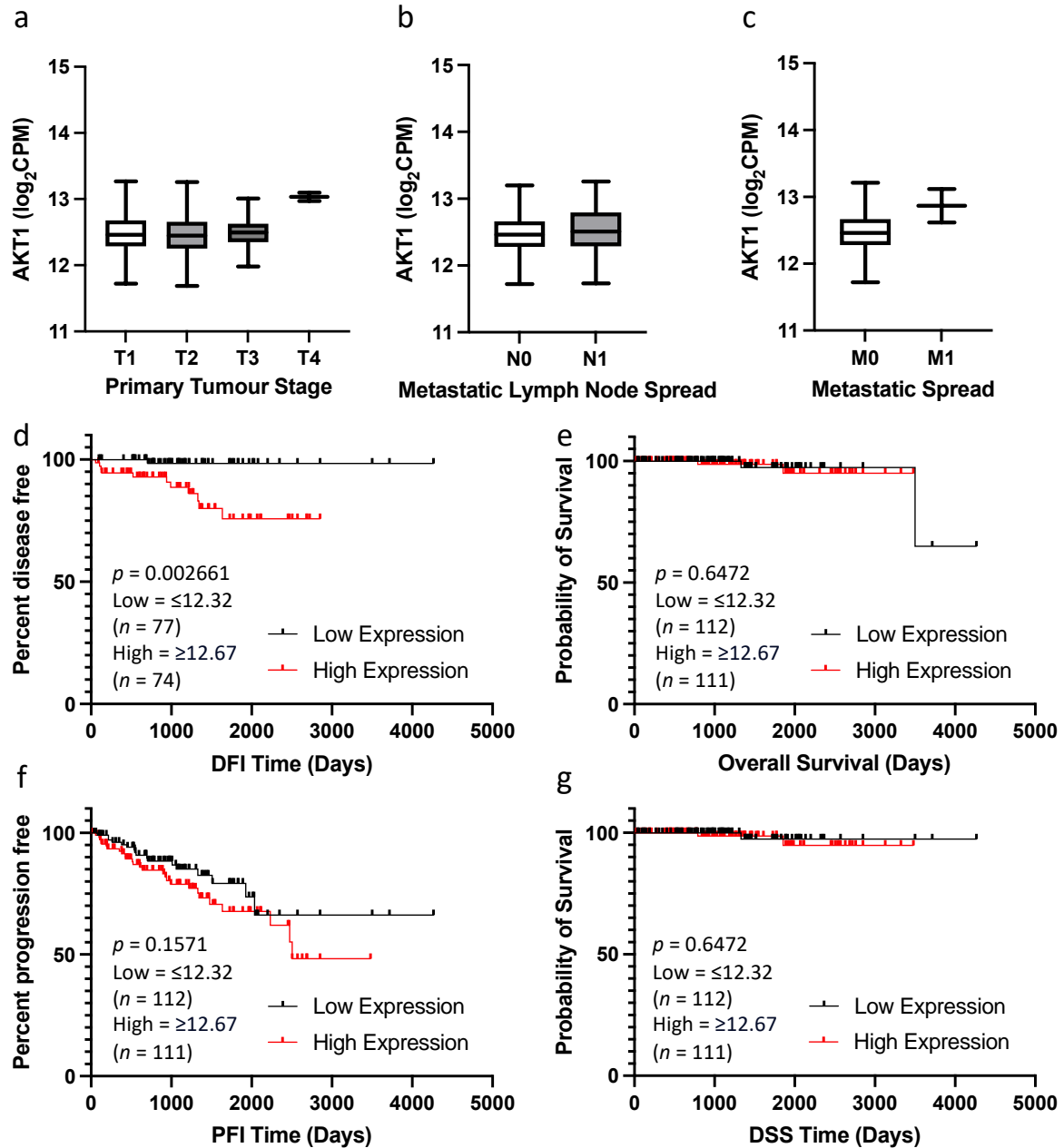


Figure S9. Correlation between AKT1 expression and clinicopathological markers of PCa progression. UCSC Xena analysis of TCGA PRAD samples shows AKT1 expression in (a) primary tumour stage, T1 ($n = 152$), T2 ($n = 164$), T3 ($n = 50$) and T4 ($n = 2$), (b) metastatic lymph node spread, N0 ($n = 302$) and N1 ($n = 65$) and (c) metastatic spread M0 ($n = 365$) and M1 ($n = 2$). For KM plots, patients were divided into quartiles based on AKT1 expression. (d) High expression of AKT1 was associated with significantly reduced DFI, Low = ≤ 12.32 ($n = 77$), High = ≥ 12.67 ($n = 74$). (e) No significant difference was observed between AKT1 expression and overall survival, Low = ≤ 12.32 ($n = 112$), High = ≥ 12.67 ($n = 111$) (f) No significant difference was observed between AKT1 expression and DSS, Low = ≤ 12.32 ($n = 112$), High = ≥ 12.67 ($n = 111$). (g) No significant difference was observed between AKT1 expression and PFI, Low = ≤ 12.32 ($n = 112$), High = ≥ 12.67 ($n = 111$). p -values for KM plots generated via log-rank (Mantel-Cox) tests. CPM = Copies per million; n = number; DFI = disease free interval; DSS = disease specific survival; PFI = Progression free interval.

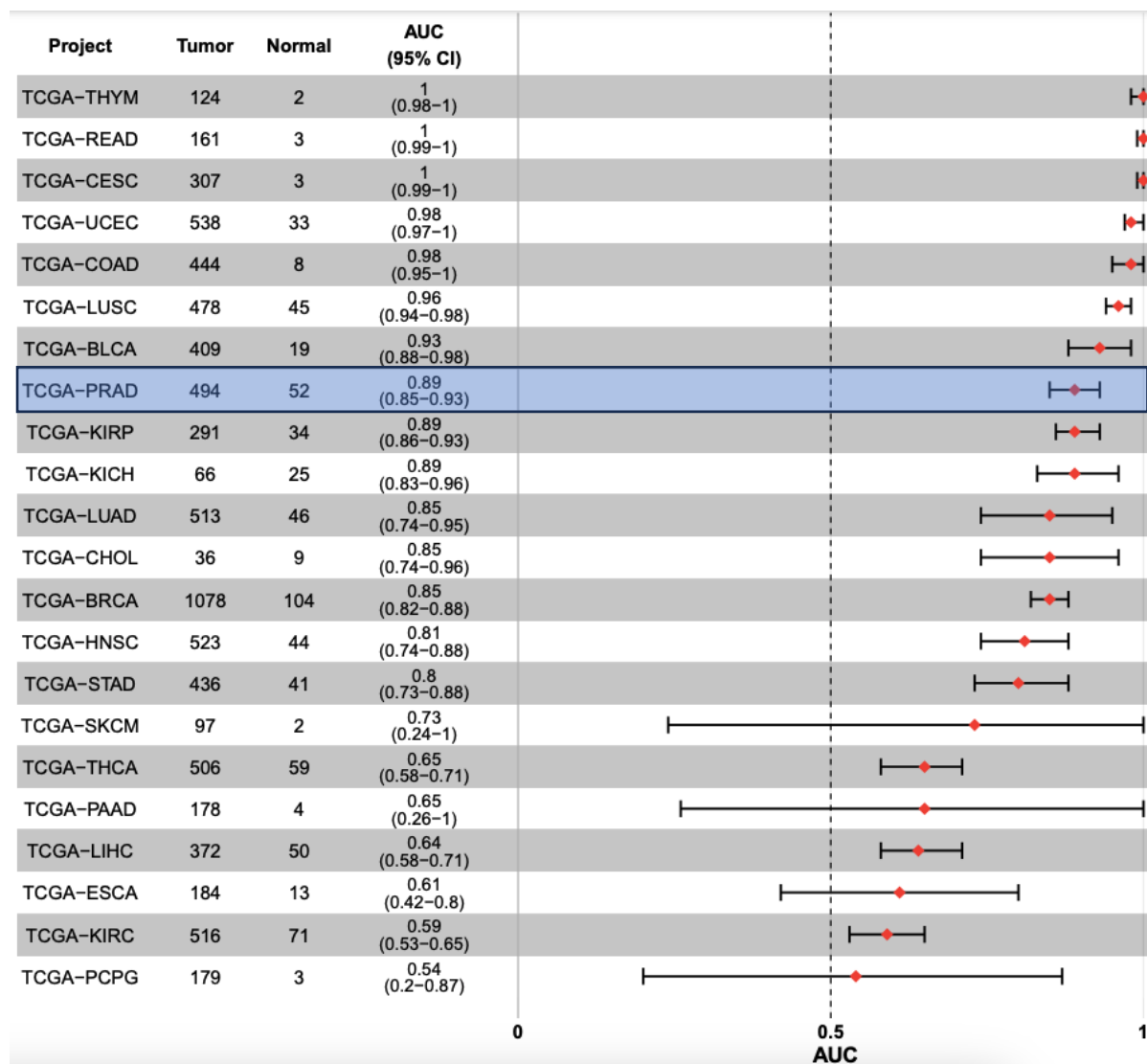


Figure S10. CancerMIRNome TCGA Pan- Cancer ranked forest plots of miR-143-3p ROC analysis shows miR-143-3p has significant diagnostic value in multiple cancer types. Result for prostate cancer is enclosed in the blue box (TCGA-PRAD).

Table S1. KM plotter meta-analysis results of overall survival in various cancers comparing high/low expression of AKT1 and miR-143. Only cancers for which log-rank $p < 0.05$ are presented. HR estimated for high compared to low expression (Cox proportional analysis, auto-selected cut-off).

| | <i>Cancer</i> | <i>n</i> | <i>HR*</i> | <i>Log-rank p-value</i> |
|-------------------|---------------------------------------|----------|------------|-------------------------|
| <i>AKT1</i> | Breast cancer | 1089 | 1.45 | 0.0308 |
| | Cervical squamous cell carcinoma | 304 | 1.69 | 0.0427 |
| | Oesophageal Adenocarcinoma | 80 | 0.26 | 0.0001 |
| | Head-neck squamous cell carcinoma | 499 | 1.42 | 0.0098 |
| | Kidney renal papillary cell carcinoma | 287 | 0.45 | 0.0292 |
| | Liver hepatocellular carcinoma | 370 | 1.7 | 0.0025 |
| | Lung adenocarcinoma | 504 | 0.7 | 0.0202 |
| | Ovarian cancer | 373 | 0.65 | 0.0031 |
| | Pancreatic ductal adenocarcinoma | 177 | 0.6 | 0.0305 |
| <i>miR-143-3p</i> | Bladder Carcinoma | 408 | 1.75 | 0.0002 |
| | Head-neck squamous cell carcinoma | 522 | 1.37 | 0.0196 |
| | Kidney renal clear cell carcinoma | 516 | 0.71 | 0.0224 |
| | Kidney renal papillary cell carcinoma | 290 | 2.77 | 0.0005 |
| | Pancreatic ductal adenocarcinoma | 178 | 2.06 | 0.0007 |
| | Sarcoma | 259 | 0.61 | 0.0334 |

* Red text indicates HR > 1; high expression of miR-143 or AKT1 predicted poor prognosis; blue text indicates HR < 1; low expression of miR-143-3p or AKT1 predicted favourable prognosis. n = number; HR = Hazard ratio; KM = Kaplan-Meier